THE JOURNAL OF PHYSICAL CHEMISTRY C

Article

pubs.acs.org/JPCC

Ab Initio Investigation of Polyethylene Glycol Coating of TiO_2 Surfaces

Daniele Selli* and Cristiana Di Valentin*

Dipartimento di Scienza dei Materiali, Università di Milano-Bicocca, via Cozzi 55 20125 Milano, Italy

Supporting Information

ABSTRACT: In biomedical applications, TiO_2 nanoparticles are generally coated with polymers to prevent agglomeration, improve biocompatibility, and reduce cytotoxicity. Although the synthesis processes of such composite compounds are well established, there is still a substantial lack of information on the nature of the interaction between the titania surface and the organic macromolecules. In this work, the adsorption of polyethylene glycol (PEG) on the TiO_2 (101) anatase surface is modeled by means of dispersion-corrected density functional theory (DFT-D2) calculations. The two extreme limits of an infinite PEG polymer $[-(OCH_2CH_2)_n]$, on one side, and of a short PEG dimer molecule $[H(OCH_2CH_2)_2OH]$, on the other, are analyzed. Many different molecular configurations and modes of adsorption are compared at increasing surface coverage densities. At low and medium coverage, PEG prefers to lay down on the surface, while at full coverage, the adsorption is maximized when PEG molecules bind perpendicularly to the surface and interact with each other through lateral dispersions, following a mushroom to brush transition. Finally, we also consider the adsorption of competing water molecules at different coverage densities, assessing whether PEG would remain bonded to the surface or desorb in the presence of the aqueous solvent.

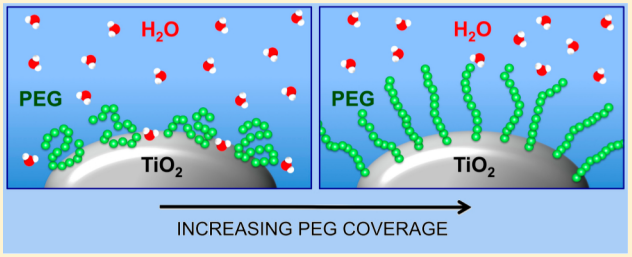

1. INTRODUCTION

Titanium oxide is the most important Ti compound and the most studied metal oxide due to its disparate technological applications. It shows unique features,[1] and it is widely used in a variety of fields, such as in the pigment industry, as a gas sensor,[2] in water photolysis,[3] as a protective agent from corrosion,[4] for photocatalytic decontamination,[5] in photoelectrochemistry,[6,7] for hydrogen production,[8] and more recently in many biomedical applications.[9] Rutile is the most stable titanium oxide allotrope at ambient conditions; however, it has been demonstrated that TiO_2 nanoparticles with sizes suitable for medical applications (generally below 20 nm) prefer the anatase phase.[10] Although TiO_2 nanoparticles are extremely promising in the biomedical field, since they could be used for imaging[11] and sonodynamic[12] or photodynamic[13] therapy of cancer, it has been recently shown that, contrary to biologically inert bulk TiO_2, nanoparticles are extremely cytotoxic[14,15] and have to be pretreated to be safely used in a clinical context.[16]

Thus, it is not surprising that in recent years the interaction between TiO_2 (101) anatase surface, the most exposed surface of faceted TiO_2 nanoparticles (NPs),[17] and biologically relevant molecules has been largely investigated by the theoretical community.[18−22] The dynamic adsorption of single water molecules and multiple water layers has been exhaustively pointed out in different works based on Car-Parrinello molecular dynamics simulations.[23,24] How methanol (the simplest alcohol), formic acid (the simplest organic acid), and other organic small adsorbates interact with the (101) anatase surface has been investigated in other DFT theoretical studies.[20,22,25] Furthermore, molecular dynamics simulations based on classical force fields and ab initio calculations have been exploited to model the interaction of TiO_2 surfaces with simple amino acids like glycine, arginine, lysine, aspartic acid,[26−28] or slightly more complex peptides usually present in the cytoplasmic matrix.[29]

Polymer coating of nanoparticles (NPs) is considered as the most effective approach to control their physical features, such as solubility and size, to regulate their mobility and penetration of tissues, and to keep their level of toxicity low. Grafting of polyethylene glycol (PEG) chains is usually the best way to cover NPs, since PEG is an FDA-approved, versatile, inexpensive, and well-known polymer and NPs PEGylation is a well-established process.[16,30] It prevents their agglomeration[31] and gives "stealth" properties to the nanocarrier;[32,33] PEG has favorable pharmacokinetics and tissue distribution[34] and reduces the uptake by a reticuloendothelial system (RES), increasing the in vivo circulation time.[35] However, water and different organic or biological molecules present in the human body can compete with PEG adsorption and reduce the long-term stability of PEG/TiO_2 nanohybrids.

In this work, we address this problem from a computational point of view by modeling the PEG/TiO_2 surface interaction. We calculate the adsorption energies, in vacuo, for various

Received: September 21, 2016
Revised: October 24, 2016
Published: October 25, 2016

DOI: 10.1021/acs.jpcc.6b09554
J. Phys. Chem. C 2016, 120, 29190−29201

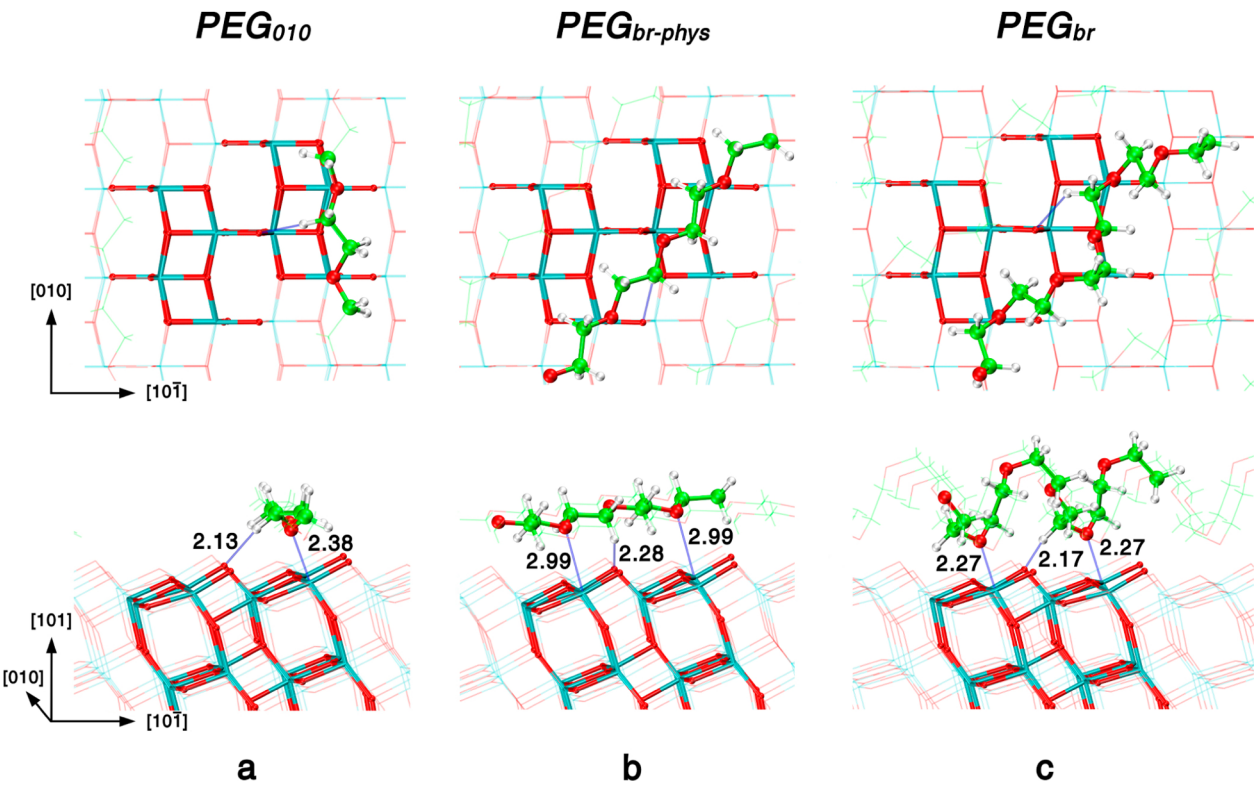

Figure 1. Optimized structures of infinite PEG chains on the TiO_2 (101) anatase surface (Table 1). (a) Chain is deposited along a Ti_{5c} row of the surface (PEG_{010}). (b) Polymer weakly physisorbs on the surface crossing different Ti_{5c} rows over bridging O_{2c} sites ($PEG_{br\text{-}phys}$). (c) Higher number of monomers per supercell allows the chain for rippling and binding Ti_{5c} atoms on different rows (PEG_{br}). Distances in Å.

equilibrium geometries of both infinitely long PEG polymers $[-(OCH_2CH_2)_n]$ and short PEG dimer molecules $[H-(OCH_2CH_2)_2OH]$ adsorbed on the TiO_2 (101) anatase surface by means of DFT-D2 calculations. The Grimme's approach (D2)[36] is used to take into account the van der Waals interactions, which are crucial in this kind of large hybrid systems. We investigate different coverage densities, in order to mimic the usual experimental situation of a mushroom to brush transition,[37] and we compare our results with the relative adsorption energies obtained for water adsorption. Our atomistic insight allows for the detailed description of the surface-adsorbate interaction, usually not accessible experimentally, while comparison with the adsorption of water molecules give us a first assessment of the coating-desorption risk in an aqueous medium.

2. COMPUTATIONAL DETAILS

In all calculations, conjugate-gradient relaxations were performed by means of density functional theory within generalized gradient approximation (GGA) using the PBE functional.[38] Electron-ion interactions were described by ultrasoft pseudopotentials.[39] For all of the DFT geometry optimizations, the open-source simulation package Quantum ESPRESSO has been used.[40] Plane-wave basis set cutoffs for the smooth part of the wave functions and the augmented density were 30 and 300 Ry, respectively. A Monkhorst-Pack k-point mesh of 2 × 2 × 1 ensured the convergence of the electronic part. Forces were relaxed to less than 0.005 eV/Ang. Long-range van der Waals interactions have been taken into account including a semiempirical dispersion correction in the GGA density functional, as reported in the study of Grimme (DFT-D2).[36]

The TiO_2 (101) anatase surface has been modeled with a three triatomic layer slab, where the atoms of the bottom layer were kept fixed to the bulk position during all relaxations to ensure the rigidity of the surface. Periodic replicas were separated by 20 Å of vacuum in the direction perpendicular to the surface, while two different slab supercell models, 1 × 2 or 1 × 3, were considered for modeling the adsorption of an infinite PEG polymer or water and the PEG dimer molecules, respectively.

For infinite PEG chains (obtained by repeating a PEG portion with the supercell periodic boundary conditions), the total adsorption energy has been evaluated with the following equation

$$\Delta E_{ads} = E_{slab+pol} - (E_{slab} + nE_{mon}) \quad (1)$$

where $E_{slab+pol}$ is the energy of the whole system, i.e., the TiO_2 surface slab and the polymer chain adsorbed on it, and E_{slab} is the energy of the surface slab alone. As the reference energy for the PEG portion (E_{mon}), we take half the energy of a fully relaxed, periodically repeated, PEG dimer in the gas phase. n is the number of monomers constituting the PEG chain (n = 2, 4, or 6 in our models; see section 3.1). To compare adsorption energy values for PEG chains of different lengths, we also defined the energy per monomer $-(OCH_2CH_2)$ as follows:

$$\Delta E_{ads}^{mon} = \Delta E_{ads}/n \quad (2)$$

Water or PEG dimer molecules have been arranged in different positions on the surface and at different coverage densities. The total adsorption energy is computed according to the following equation

$$\Delta E_{ads} = E_{slab+nmol} - (E_{slab} + n_{mol}E_{mol}) \quad (3)$$

DOI: 10.1021/acs.jpcc.6b09554
J. Phys. Chem. C 2016, 120, 29190−29201

where $E_{slab+nmol}$ is the energy of the whole system, i.e., the TiO_2 surface slab and all the molecules adsorbed on it, E_{slab} is the energy of the surface slab alone, E_{mol} is the energy of an isolated undissociated molecule in the gas phase, and n_{mol} is the number of molecules.

We also defined the adsorption energy per molecule

$$\Delta E_{ads}^{mol} = \frac{\Delta E_{ads}}{n_{mol}} \quad (4)$$

when more than one molecule are present in the repeating supercell.

For both the infinite PEG chains and the PEG dimer molecules, it is useful to determine the adsorption energy per active site

$$\Delta E_{ads}^{site} = \frac{\Delta E_{ads}}{n_{site}} \quad (5)$$

since they may bind more than one adsorption site per chain or per molecule. n_{site} is the total number of occupied adsorption sites. On the anatase (101) surface, the adsorption sites are the 5-fold coordinated Ti atoms, which are four in the case of the 1 × 2 surface supercell and six in the case of the 1 × 3. Note also that the superficial 2-fold coordinated O atoms, connecting Ti atoms of different rows, can be involved in the adsorption process of molecules since they represent active sites for possible H-bonds, as we will discuss in the following section.

3. RESULTS AND DISCUSSION

The paper is organized as follows: we present the adsorption of infinite PEG chains in section 3.1; we present the adsorption of PEG dimer molecules at various coverages (low, medium, and full) in section 3.2; in section 3.3, we illustrate and discuss the energy contribution to the adsorption energy in terms of deformation, binding, and intermolecular energies; finally, in section 3.4, we compare the adsorption energies of infinite PEG chains and of PEG dimer molecules with those for water up to a complete monolayer level of coverage in order to assess whether, in an aqueous environment, water molecules can compete with the polymer and eventually cause its desorption.

3.1. Infinite PEG Chain Adsorption. The chemically active sites of the (101) anatase surface are the 5-fold coordinated cationic Ti atoms (Ti_{5c}) and the 2-fold coordinated anionic O atoms (O_{2c}). PEG compound is generally made of rather long polymer chains: ideally, one can imagine them as infinite chains. In our adsorption models, we have first deposited a portion of a PEG chain on top of a 1 × 2 supercell of the titania surface with two different orientations, and then we have applied the periodic boundary conditions, which result in an ideally infinite bidimensional anatase (101) surface and an ideally infinite monodimensional polymer.

In the first orientation, the PEG was laid horizontally and its chain axis was aligned with a Ti_{5c} atom row, i.e., along the [010] direction (Figure 1a, PEG_{010}). In this case, two PEG monomers are required to fit the lattice distance of the 1 × 2 TiO_2 supercell model used. Each oxygen atom of the PEG binds weakly with a Ti_{5c} atom of the surface, while the H atoms of the ethylene moiety interacts with the O_{2c}.

In the second orientation, the PEG molecule lays again horizontally but across different Ti_{5c} rows, along a direction that is rotated about 45° clockwise with respect to the [010] direction (Figure 1b, $PEG_{br\text{-}phys}$). Here, at least four PEG monomers are required to fit the supercell distance: one oxygen atom of the chain binds the Ti_{5c} of a row, the next one is in bridging position above the O_{2c} atom of the surface (Figure 1b), and the next is, again, on a Ti_{5c} of another parallel Ti_{5c} row, etc. In this orientation, no chemical bond is formed, but the polymer chain is rather physisorbed, standing at about 3 Å above the surface. In order to observe the formation of proper chemical bonding in the second orientation, six PEG monomers should be considered to allow for the rippling of the chain (see Figure 1c, PEG_{br}): one oxygen atom binds the Ti_{5c} of a row, the next two are in bridging position above the O_{2c} atom of the surface and then, next binds a Ti_{5c} of another parallel Ti_{5c} row.

Values of the total adsorption energy and adsorption energy per site and per monomer for all of the orientations and configurations described above are reported in Table 1. Note that in all three cases the PEG chain interacts with two Ti_{5c} adsorption sites.

Table 1. Total Adsorption Energy, Adsorption Energy per Site and per Monomer (Expressed in eV) for the Infinite PEG Chain Oriented Parallel to a Ti_{5c} Row of the (101) Anatase Surface (PEG_{010}) or across the Bridging O_{2c} Row ($PEG_{br\text{-}phys}$ and PEG_{br})[a]

	ΔE_{ads}	ΔE_{ads}^{site}	ΔE_{ads}^{mon}
PEG_{010}	−0.45	−0.22	−0.22
$PEG_{br\text{-}phys}$	+0.46	+0.23	+0.11
PEG_{br}	−1.95	−0.98	−0.33

[a]Representations of the optimized structures are reported in Figure 1.

In the case of PEG_{010}, although the chain is quite stretched in order to fit the lattice parameter of anatase TiO_2 (strain-energy cost per monomer of 0.51 eV), the stabilization coming from the chemical interaction with the surface and the dispersion forces is sufficiently large to reach the thermodynamic stability (see Table 1). On the contrary, the $PEG_{br\text{-}phys}$ is not stable. The PEG chain is largely stretched (strain-energy cost per monomer of 0.39 eV), too, with no compensating chemical bond formed but only weak dispersion forces. As mentioned above, only the six PEG monomer model (PEG_{br} in Figure 1c) allows the rippling and an arrangement where the PEG O atoms chemically bind to the Ti_{5c} of the anatase surface (see Table 1). Larger intramolecular weak dispersion interactions within the polymer chain in PEG_{br} are probably the reason for an extra stabilization of ∼0.1 eV per monomer with respect to the PEG_{010} case.

We may conclude this part of the work with the consideration that the stretched models PEG_{010} and $PEG_{br\text{-}phys}$ are probably nonrealistic to describe long PEG chains on TiO_2 surface, whereas from the PEG_{br} model we learn that long chains will spontaneously fold when deposited on a TiO_2 surface.

3.2. PEG Dimer Molecule Adsorption. In this section, we consider the adsorption of a short PEG chain (just two repeating units, a dimer D molecule) on the TiO_2 (101) anatase surface. The molecule has both terminal oxygens saturated with H atoms forming OH groups. Since the coverage strongly influences the way the PEG polymer arranges on flat or curved TiO_2 surfaces, we have investigated three different levels of coating: the low, medium, and full coverage regimes. In parallel, we have considered three different possible orientations of the dimer molecule on the TiO_2 surface: parallel to the surface plane and to the Ti_{5c} rows (D_{010}, Figure

DOI: 10.1021/acs.jpcc.6b09554
J. Phys. Chem. C 2016, 120, 29190−29201

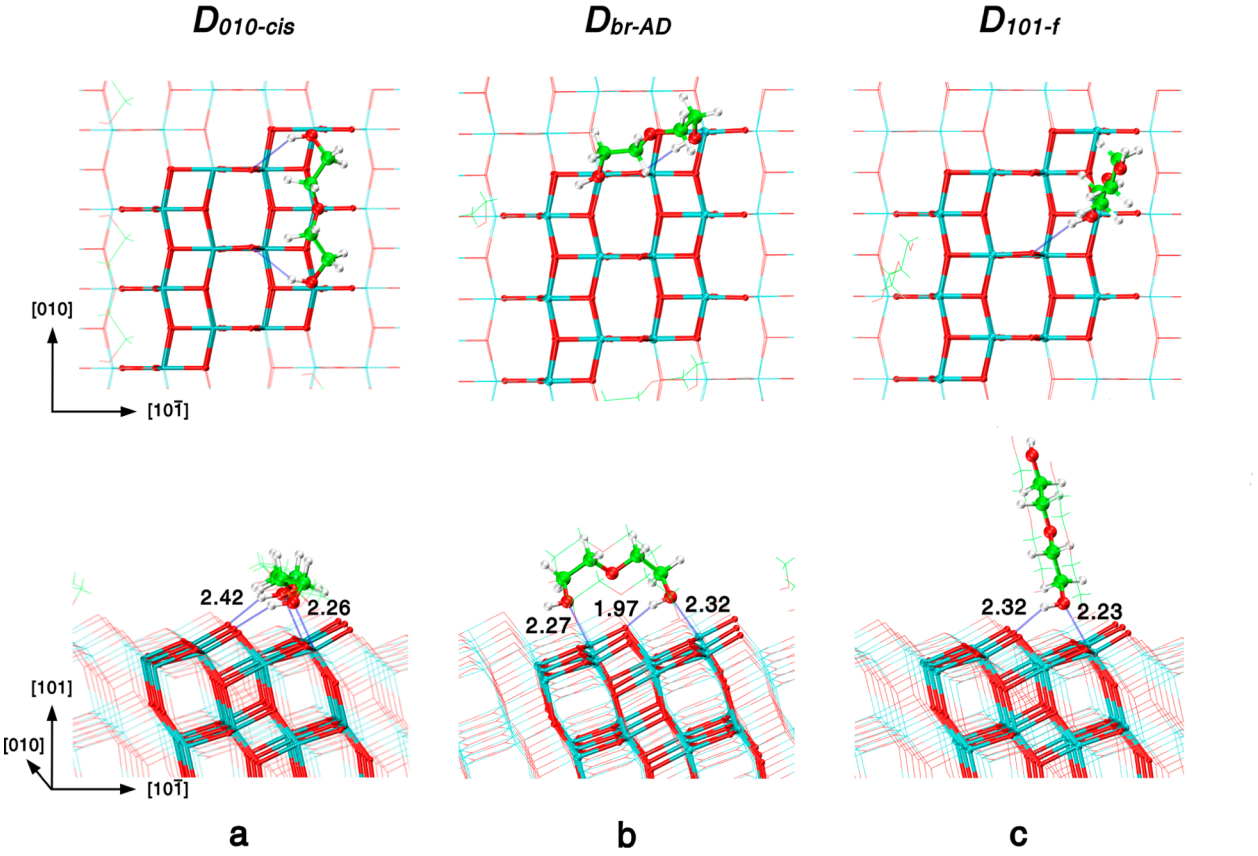

Figure 2. Optimized structures for the adsorption of an undissociated PEG dimer molecule onto the TiO_2 (101) anatase surface slab model (Table 2 and Table 1S). Only the most stable configurations are shown. (a) PEG dimer molecule lays down along a row of Ti_{5c} atoms in the $D_{010\text{-}cis}$ configuration. (b) PEG dimer molecule is deposited across two Ti_{5c} rows in the bridging $D_{br\text{-}AB}$ configuration. (c) PEG dimer molecule is perpendicular to the surface on top of a Ti_{5c} atom in a $D_{101\text{-}f}$ configuration. Distances in Å.

Table 2. Total Adsorption Energy and Adsorption Energy Per Site (Expressed in eV) for Undissociated, Mono-, and Bi-dissociated PEG Dimer Molecules Adsorbed onto the TiO_2 (101) Anatase Slab Model[a]

			Low Coverage					
			molecular		monodissociated		bidissociated	
	no. of D per cell	% of occ Ti_{5c} sites	ΔE_{ads}	ΔE_{ads}^{site}	ΔE_{ads}	ΔE_{ads}^{site}	ΔE_{ads}	ΔE_{ads}^{site}
$D_{010\text{-}cis}$	1	50	−1.88 (−0.94)	−0.63 (−0.31)	−1.79	−0.60	−1.68	−0.56
$D_{010\text{-}trans}$	1	50	−1.82	−0.61	−1.77	−0.59	−1.68	−0.56
$D_{br\text{-}AD}$	1	33	−1.82 (−1.16)	−0.91 (−0.56)	−1.94	−0.97	−1.98	−0.99
$D_{br\text{-}BF}$	1	33	−1.23	−0.61	−1.18	−0.59	−1.18	−0.59
$D_{101\text{-}f}$	1	16	−0.99 (−0.64)	−0.99 (0.64)	−0.78	−0.78	NA	NA
$D_{101\text{-}n}$	1	16	−0.88	−0.88	−0.74	−0.74	NA	NA

[a]Parallel to the surface plane and to a Ti_{5c} row (D_{010}), parallel to the surface plane but crossing Ti_{5c} rows (D_{br}) and perpendicular to the surface plane (D_{101}). Since in D_{101} only one −OH group interacts with the surface, bidissociation in not applicable (NA). The adsorption energy values obtained without enabling the van der Waals dispersion corrections are shown in parentheses. Representations of the optimized structures are reported in Figure 2, Figure 4, and Figures 2S and 3S.

2a), parallel to the surface plane but crossing the Ti_{5c} rows (D_{br}, Figure 2b), and perpendicular to the surface plane (D_{101}, Figure 2c).

3.2.1. Low Coverage. To describe a low coverage regime we have used an anatase (101) 1 × 3 supercell surface model with six active Ti_{5c} sites. Depending on the orientation of the adsorbed dimer, the coverage density, defined as the % of occupied Ti_{5c} sites, differs. For D_{010} it corresponds to 50%, since the molecule interacts with three Ti_{5c} sites along a row in the [010] direction, for D_{br} it is 33%, with two Ti_{5c} sites, in different [010] rows, involved in the interaction, and for D_{101} it is 16%, with just one Ti_{5c} site involved in the interaction with the dimer molecule (see Figure 2). Note that, in the low coverage regime, $\Delta E_{ads}^{mol} = \Delta E_{ads}$, since only one PEG dimer molecule (D) is considered per repeating supercell.

For a given dimer orientation, e.g., D_{010}, more possible configurations are conceivable. For instance, the central ethereal O atom can point upward or downward. However, full atomic relaxation showed that only the latter configuration is stable. Then, both terminal OH groups could point toward the closest (on the right) or the farthest (on the left) O_{2c} bridging atoms of the surface (*cis*), or one could point in one

DOI: 10.1021/acs.jpcc.6b09554
J. Phys. Chem. C 2016, 120, 29190−29201

direction and the other OH group could point in the opposite direction (*trans*) (compare Figure 2a with Figure 1Sa). The most favorable configuration is the *cis* pointing toward the farthest bridging O atoms, although only by ∼0.06 eV. In this case, the two terminal OH groups bind to the Ti_{5c} of the surface (Ti−O bonds) and the H atoms form weak H-bonds (length of ∼2.4 Å) with the farthest O_{2c} atom. This strongly stabilizes the molecule, leading to an adsorption energy of −1.88 eV (see Table 2). The other *cis* conformation is never found to be an equilibrium structure at low coverage, but it converts into the *trans* conformation.

For the bridging dimer D_{br}, where the PEG molecule is bonded to Ti_{5c} atoms of different rows, two different configurations are conceivable (see Figure 3). In the first case, the terminal O atoms of the molecule bind to two collinear Ti_{5c} atoms (e.g., sites A and D in Figure 3a). We call this configuration $D_{br\text{-}AD}$ (Figure 2b and blue molecule in Figure 3b).

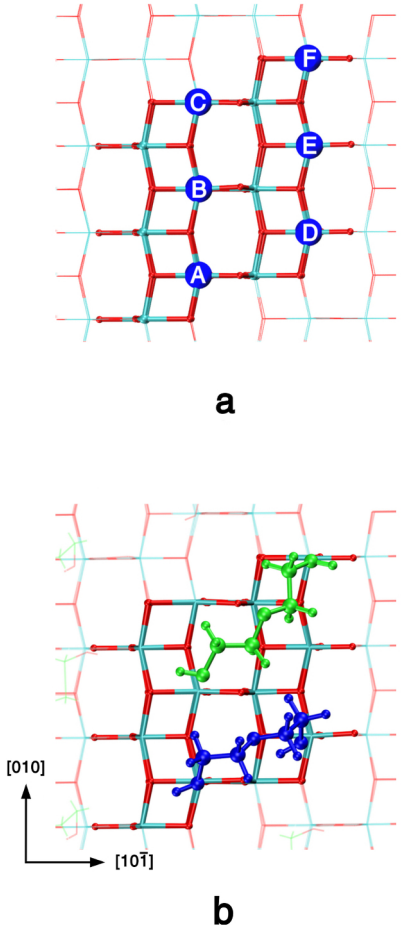

Figure 3. (a) Top view of the adsorption sites for the PEG dimer molecules. Each letter corresponds to one of the six different Ti_{5c} present in a 1 × 3 TiO_2 (101) anatase supercell. (b) Top view of two D_{br} PEG dimer molecules adsorbed on the TiO_2 (101) anatase surface. The green molecule refers to $D_{br\text{-}BF}$ and the blue one to $D_{br\text{-}AD}$.

In the second configuration, that is, the $D_{br\text{-}BF}$ (green molecule in Figure 3b), the dimer is stretched in order to allow the terminal O atoms to bind two noncollinear Ti_{5c} atoms (e.g., sites B and F in Figure 3a). $D_{br\text{-}AD}$ is more stable by ∼0.6 eV than $D_{br\text{-}BF}$ (see Table 2). This is mainly because in $D_{br\text{-}AD}$ the terminal OH groups of the PEG molecule form a strong H-bond with the O_{2c} of the surface, while in $D_{br\text{-}BF}$ the interaction of the same atoms with the closer O_{2c} is rather weak (the shortest −OH−O_{2c} distances are ∼2.65 Å). In addition, while in the $D_{br\text{-}BF}$ configuration the dimer is largely stretched (43.99% with respect to its counterpart in the gas phase), in the $D_{br\text{-}AD}$ the elongation is much less strong (5.36%).

The last configurations considered in the low coverage regime are the ones where the PEG molecule binds perpendicular to the anatase (101) surface (D_{101}). This should mimic the experimental situation where only one extremity of the polymer is grafted to the surface. Two binding modes are possible: with the H of the terminal hydroxyl bonded to the Ti_{5c} of the surface pointing toward either the nearest O_{2c}, $D_{101\text{-}n}$ (Figure 1Sc), or the farthest O_{2c} atom, $D_{101\text{-}f}$ (see Figure 2c). We found that $D_{101\text{-}f}$ is more stable by −0.12 eV (see Table 2), in agreement with a previous theoretical work[22] on simpler alcohols interacting with the TiO_2 (101) anatase surface.

Note that in Figure 2 only the most stable configuration per dimer molecule orientation is shown. The other configurations are reported in Figure 1S.

As a next step, we have investigated the possibility of mono and bidissociation of the terminal OH groups of the PEG dimer molecules. $D_{010\text{-}cis}$, $D_{br\text{-}AD}$, and $D_{101\text{-}f}$ are more stable configurations than $D_{010\text{-}trans}$, $D_{br\text{-}BF}$, and $D_{101\text{-}n}$, respectively, also in the dissociated state, as detailed in Table 2. Several other possible destinations of the dissociated protons or different OH dissociation were considered, besides the most stable ones reported in Table 2 and Figure 4. Those are described in Table 1S and Figures 2S and 3S.

In the case of $D_{010\text{-}cis}$, the mono- (see Figure 4a) or bidissociated (see Figure 3Sa) dimer molecules are not favored with respect to the molecular form. The energy cost for the first dissociation is 0.09 eV (from −1.88 to −1.79 eV), whereas for the second it is 0.11 eV (from −1.79 to −1.68 eV). Thus, in the next sections, $D_{010\text{-}cis}$ will always be considered as undissociated.

The situation is different for $D_{br\text{-}AD}$. The first OH dissociation induces a gain of −0.15 eV in the adsorption energy. There is a tiny further stabilization if both OH groups dissociate −0.02 eV. We must note that the mono- and bidissociated $D_{br\text{-}AD}$ forms are the most stable among all the configurations for an adsorbed PEG dimer molecule considered in this work (see Table 2 and Table 1S). This is because, in addition to the chemical bonds between the terminal oxygen atoms of the PEG dimer molecule and the Ti_{5c} of the surface (∼1.8 Å), a strong H-bond between the central O of the PEG dimer molecule and the dissociated H atom, now bonded to an O_{2c} of the surface (O_{2c}H), is also established (1.69 Å, see Figure 4b). The possibility that the dissociated H atom/atoms migrate from the closest O_{2c} atom to other further apart O_{2c} sites has been investigated, but no stabilization was observed (see Table 1S and Figures 2Sb and 3Sc).

On the contrary, if the PEG molecule is in a stretched bridging configuration between two Ti_{5c} atom rows, $D_{br\text{-}BF}$, the dissociation of the terminal hydroxyl groups does not promote the bonding of the molecule to the surface. Both the single and double dissociation (Figure 2Sc and Figure 3Sd) bring to a similar energy loss of ∼0.1 eV (see Table 2).

In the case of the standing PEG dimer molecule, $D_{101\text{-}f}$, only one OH group is in contact with the surface and is eventually capable of dissociation (see Figure 4c). However, such dissociation is not favored by ∼0.1 eV.

3.2.2. Medium Coverage. In the medium coverage regime, only the standing $D_{101\text{-}f}$ and the bridging $D_{br\text{-}AD}$ and $D_{br\text{-}BF}$

DOI: 10.1021/acs.jpcc.6b09554
J. Phys. Chem. C 2016, 120, 29190−29201

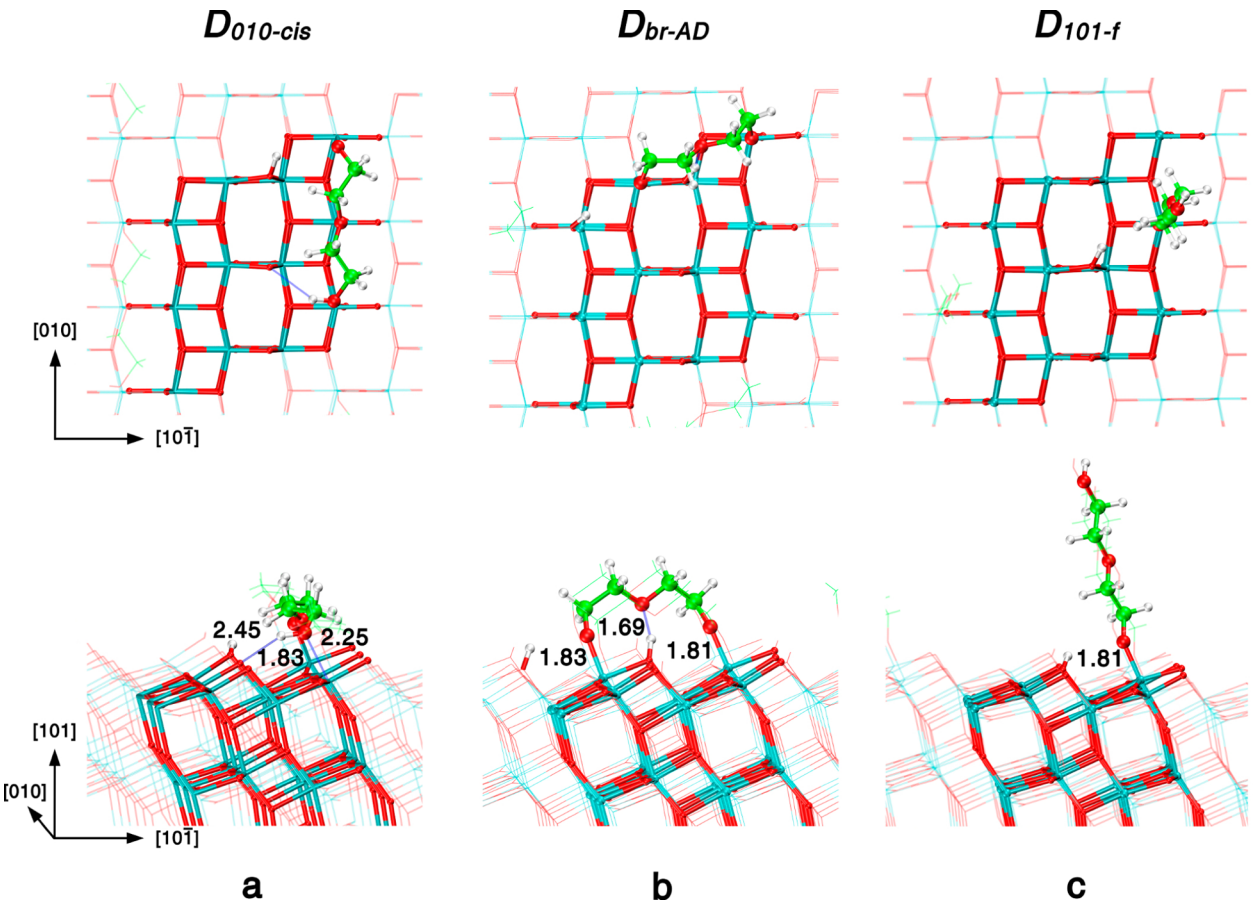

Figure 4. Optimized structures for the adsorption of a dissociated PEG dimer molecule onto the TiO_2 (101) anatase surface (Table 2 and Table 1S). Only the most stable one per adsorption mode is shown. (a) Monodissociation of a PEG dimer molecule laying down along a row of Ti_{5c} atoms in a $D_{010\text{-}cis}$ configuration. (b) Bidissociation of a PEG dimer molecule laying across two Ti_{5c} rows in the bridging $D_{br\text{-}AB}$ configuration. (c) Monodissociation of the PEG dimer molecule deposited perpendicular to the surface on top of a Ti_{5c} atom in a $D_{101\text{-}f}$ configuration. Distances in Å.

configurations have been considered. In the first case, two or three PEG dimer molecules are grafted to the surface for a coverage density (% of occupied Ti_{5c} sites) of 33% and 50%, respectively. For $D_{br\text{-}AD}$ and $D_{br\text{-}BF}$, the coverage is of 66% since two PEG dimer molecules bind four Ti_{5c} adsorption sites. All of the optimized structures for the medium coverage are reported in Figure 4S.

When two PEG dimer molecules adsorb on the surface in the standing form ($D_{101\text{-}f}$, 33% coverage density), three nonequivalent adsorption patterns exist (refer to Figure 3a for the adsorption site definition). In the $D_{101\text{-}f\text{-}BF}$ configuration, the two PEG dimer molecules are bonded on two noncollinear Ti_{5c} atoms in different rows; in the $D_{101\text{-}f\text{-}BE}$ one, the two molecules are bonded to two Ti atoms in different rows but collinear, while in the $D_{101\text{-}f\text{-}AB}$ configuration, the two PEG dimer molecules are adjacent, bonded to two Ti atoms of the same row (see Figure 4S for the equilibrium geometries). The adsorption energy in all three cases is very similar, with the $D_{101\text{-}f\text{-}BF}$ and $D_{101\text{-}f\text{-}AB}$ configurations slightly more favorable (see Table 3). This is mainly because the closer the molecules, the larger the long-range stabilizing dispersion interactions and the possibility to form H bonds with the terminal free OH groups, not bonded to the surface Ti_{5c}. The extra stabilization coming from the intermolecular dispersion interactions increases the binding energy by −0.05 eV with respect to the isolated PEG dimer molecule, $D_{101\text{-}f}$, discussed in the previous section (section 3.2.1) (when comparing different coverages refer to the adsorption energy per site ΔE_{ads}^{site}).

Table 3. Total Adsorption Energy, Adsorption Energy per PEG Dimer Molecule, and Adsorption Energy per Site (Expressed in eV) for Two or Three PEG Dimer Molecules Binding the TiO_2 (101) Anatase Surface in $D_{101\text{-}f}$ or D_{br} Configurations[a]

	Medium Coverage				
			molecular		
	no. of D per cell	% of occ Ti_{5c} sites	ΔE_{ads}	ΔE_{ads}^{mol}	ΔE_{ads}^{site}
$D_{101\text{-}f\text{-}BE}$	2	33	−1.93	−0.96	−0.96
$D_{101\text{-}f\text{-}BF}$	2	33	−2.05	−1.02	−1.02
$D_{101\text{-}f\text{-}AB}$	2	33	−2.05	−1.03	−1.03
$D_{101\text{-}f\text{-}ABC}$	3	50	−3.23	−1.09	−1.09
$D_{101\text{-}f\text{-}AEC}$	3	50	−3.52	−1.17	−1.17
$D_{br\text{-}AD}$/ $D_{br\text{-}BE}$	2	66	−3.32	−1.66	−0.83
$D_{br\text{-}AE}$/ $D_{br\text{-}BF}$	2	66	−2.14	−1.07	−0.54
$D_{br\text{-}AD}$/ $D_{br\text{-}BF}$	2	66	−2.86	−1.43	−0.71

[a]Representations of the optimized structures are reported in Figure 4S.

The extra stabilization between standing molecules is more evident when considering a higher coverage with three PEG

DOI: 10.1021/acs.jpcc.6b09554
J. Phys. Chem. C 2016, 120, 29190−29201

Table 4. Total Adsorption Energy, Adsorption Energy per PEG Dimer Molecule, and Adsorption Energy Per Site (Expressed in eV) for Two, Three, or Six PEG Dimer Molecules Binding the TiO_2 (101) Anatase Surface in $D_{010\text{-}cis}$, $D_{101\text{-}f}$, or D_{br} Configurations[a]

	Full Coverage				
			molecular		
	no. of D per cell	% of occ. Ti_{5c} sites	ΔE_{ads}	ΔE_{ads}^{mol}	ΔE_{ads}^{site}
$D_{010\text{-}cis}$	2	100	−3.36 (−1.37)	−1.68 (−0.68)	−0.56 (−0.23)
$D_{br\text{-}AD}$	3	100	−4.45 (−1.44)	−1.48 (−0.48)	−0.74 (−0.24)
$D_{101\text{-}f}$	6	100	−6.85 (−1.93)	−1.14 (−0.32)	−1.14 (−0.32)
			fully dissociated		
	no. of D per cell	% of occ Ti_{5c} sites	ΔE_{ads}	ΔE_{ads}^{mol}	ΔE_{ads}^{site}
$D_{br\text{-}AD}$	3	100	−5.02	−1.68	−0.84
$D_{101\text{-}f}$	6	100	−6.58	−1.10	−1.10
			mixed molecular/dissociated		
	no. of D per cell	% of occ Ti_{5c} sites	ΔE_{ads}	ΔE_{ads}^{mol}	ΔE_{ads}^{site}
$D_{101\text{-}f}$	6	100	−6.56	−1.09	−1.09

[a]Values for the corresponding dissociated form in the $D_{101\text{-}f}$ and D_{br} configurations are also reported. The adsorption energy values obtained without enabling the van der Waals dispersion corrections are shown in parentheses. Representations of the optimized structures are reported in Figure 5S.

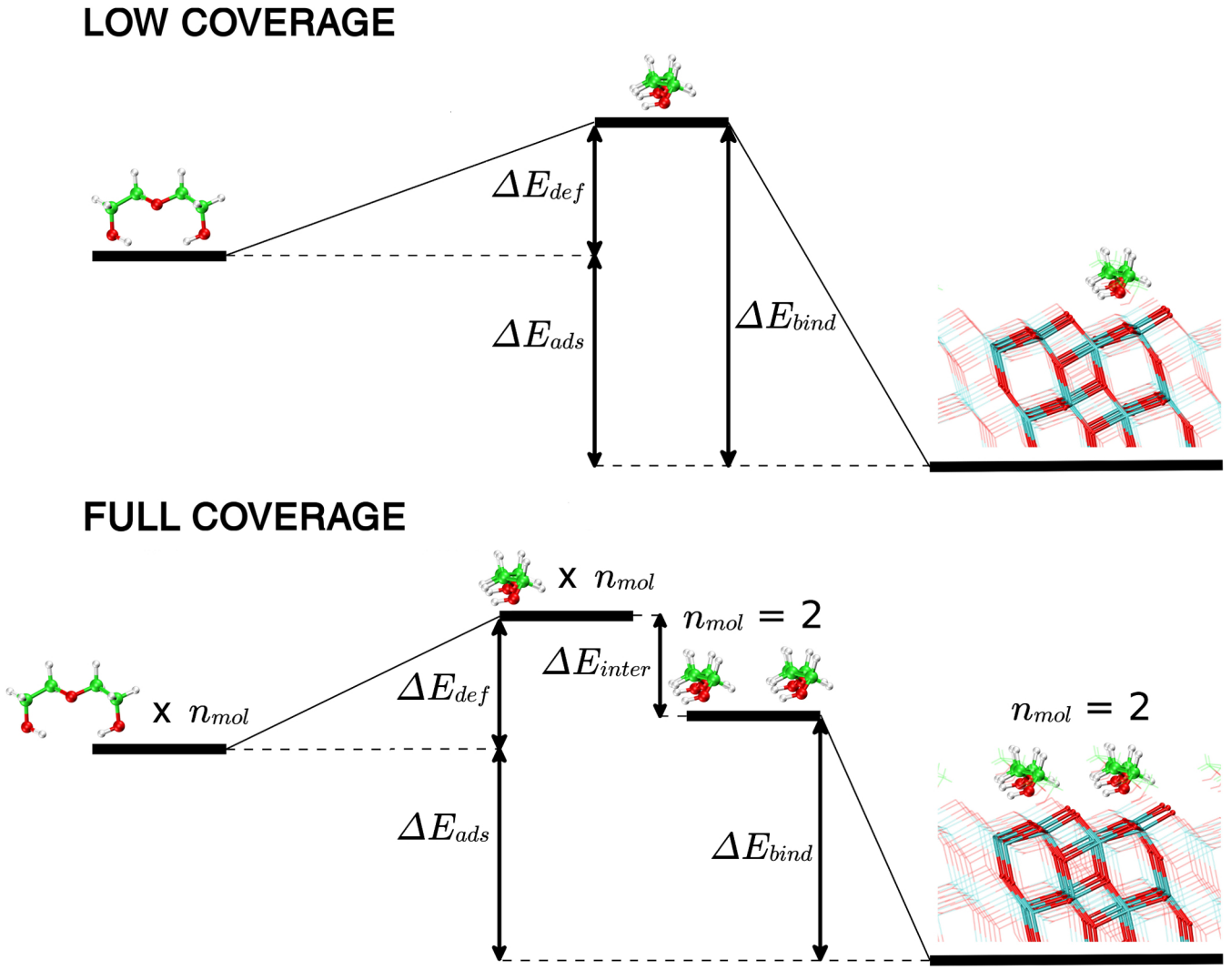

Figure 5. Schematic representation of a PEG dimer molecule adsorption process and the relative energetic contributions ($D_{010\text{-}cis}$ is used as an example). In the low coverage regime (upper panel) the gas-phase isolated PEG is first deformed (ΔE_{def}) and then allowed to bind the surface (ΔE_{bind}) with a resulting total adsorption energy (ΔE_{ads}). In the full coverage regime (lower panel), upon deformation, the PEG molecules arrange in a prebonding configuration, gaining energy from the intermolecular interactions (ΔE_{inter}). In this specific case n_{mol} = 2. In general, it is the number of molecules present in the supercell.

DOI: 10.1021/acs.jpcc.6b09554
J. Phys. Chem. C 2016, 120, 29190−29201

dimer molecules per supercell (50%). The adsorption patterns are either $D_{101\text{-}f\text{-}ABC}$ or $D_{101\text{-}f\text{-}AEC}$ (see Figure 4S). In the first case, the molecules are bonded to all the Ti_{5c} atoms of the same row and, being so close one to the other, cause an adsorption increase of about −0.1 eV per site with respect to the isolated $D_{101\text{-}f}$. In the second case, the PEG dimer molecules are staggered on Ti_{5c} atoms of different rows with a large stabilization coming from the formation of a network of H-bonds between the terminal hydroxyl groups of the PEG dimer molecules (see Figure 4S). Thus, here we have an adsorption increase of −0.18 eV per site with respect to the isolated $D_{101\text{-}f}$.

Regarding the bridgelike adsorption mode with 66% coverage density, three possible different configurations can be conceived. The two PEG dimer molecules can be either $D_{br\text{-}AD}/D_{br\text{-}BE}$ or $D_{br\text{-}AE}/D_{br\text{-}BF}$ or in a mixed configuration $D_{br\text{-}AD}/D_{br\text{-}BF}$ (see Figure 3b and Figure 4Sc). The first configuration pair is largely the most stable one, with an energy gain of about −0.3 eV per site with respect to the least one, $D_{br\text{-}AE}/D_{br\text{-}BF}$. The mixed configuration has an intermediate adsorption energy with respect to the other two (see Table 3).

As a general comment, we may notice that the standing configurations are at a largely lower energy (more stable) with respect to the bridging ones. This behavior is in contrast to what we have observed in the low coverage regime, where generally the bridging configurations (most of all the dissociated ones) were far more stable. Thus, at higher coverage density of PEG dimer molecules, long-range intermolecular interactions play a major role in the stabilization of certain configurations. This effect promotes the standing systems with respect to the configurations where the PEG dimer molecules lay down on the surface. An exhaustive discussion on how and in which measure the long-range interactions contribute to the stabilization of the various adsorption modes is presented in section 3.3.

3.2.3. Full Coverage. When all of the possible Ti_{5c} adsorption sites are involved in a chemical bond with the PEG dimer molecules, 100% coverage density is achieved. The full coverage for the $D_{010\text{-}cis}$ configuration consists of two PEG molecules laying down along the two Ti_{5c} rows on the TiO_2 surface slab model. For the fully covered bridging case, we considered three PEG dimer molecules binding AD, BE, and CF sites, respectively (see Figure 3a for labeling). Finally, six standing undissociated molecules make up the full coverage of the $D_{101\text{-}f}$ configuration. The full coverage equilibrium structures are reported in Figure 5S, whereas the energetics of adsorption are detailed in Table 4.

The adsorption energy per site for $D_{101\text{-}f}$ is quite higher than that for $D_{br\text{-}AD}$ (by −0.4 eV) and for $D_{010\text{-}cis}$ (by −0.6 eV), indicating again the tendency of the system to prefer the standing configuration at high PEG coverage.

We should recall that, at the low coverage regime (section 3.2.1), the situation is almost totally inverted (see Table 2), with the bridging $D_{br\text{-}AD}$ and $D_{010\text{-}cis}$ having adsorption energies comparable to the standing $D_{101\text{-}f}$ when considered per site but much higher when considered per PEG dimer molecule.

Thus, from a simple analysis on a thermodynamic basis, we may conclude that, at low coverage, the configurations where the PEG dimer molecules lay down on the surface are preferable to the standing cases, while at full coverage, the opposite is true. This is in line with what happens in reality, where at low coverage, polymers usually arrange in a mushroom configuration, while at high densities, the polymer prefers the so-called brush configuration.[41]

In Table 4, values of the adsorption energy for fully dissociated and mixed molecular/dissociated configurations of PEG dimer molecules are reported. For the standing case, we first consider a full dissociation of the binding OH terminal groups (100%) and then a partial dissociation where only hydroxyl groups in alternate dimers are split (50%). Such dissociations do not induce any further stabilization, in line with what was calculated for the isolated $D_{101\text{-}f}$ in section 3.2.1. In the bridging mode, when all the three PEG chains are doubly dissociated, an energy gain of about −0.2 eV per dimer is observed, in analogy to the isolated $D_{br\text{-}AD}$ analyzed in section 3.2.1. The equilibrium structures for these cases are also reported in Figure 5S.

3.3. Energy and Dispersion Contributions to the Adsorption Process. In this section, we first discuss the different energetic contributions involved in the adsorption process of the PEG dimer molecules. Then, for some selected cases, we evaluate the dispersion correction contribution.

3.3.1. Energy Contributions. In Figure 5, we report a schematic plot of the energy decomposition in the adsorption process of PEG dimer molecules, in the low (top) and full (bottom) coverage regime, on the anatase TiO_2 (101) surface. The $D_{010\text{-}cis}$ system is shown as an example, but the same scheme would correctly describe the PEG dimer molecule adsorption also in the other two configurations, $D_{br\text{-}AD}$ and $D_{101\text{-}f}$.

For the low coverage density, the adsorption process can be virtually divided in two subsequent steps: (1) the PEG dimer molecule distorts from its ideal gas-phase geometry in the deformed adsorption-adapted geometry with an energy cost (ΔE_{def}), and (2) the distorted PEG dimer molecule adsorbs forming a chemical bond with the surface, with a corresponding energy gain of binding (ΔE_{bind}). The final overall adsorption energy, per PEG molecule, is computed as

$$\Delta E_{ads}^{mol} = \Delta E_{ads} = \Delta E_{bind} + \Delta E_{def} \quad (6)$$

By analysis of the contributions obtained for the various configurations, as reported in Table 5 (upper panel), we may conclude, once again, that in the low coverage regime the PEG dimer molecule prefers to arrange parallel to the surface, instead of binding perpendicularly, even if this costs a larger distortion energy (ΔE_{def}). Although the final adsorption energy for $D_{010\text{-}cis}$ and $D_{br\text{-}AD}$ is very similar, with the $D_{010\text{-}cis}$ configuration slightly favored, the energy needed to deform the gas-phase PEG dimer molecule in the $D_{010\text{-}cis}$ prebonding

Table 5. Energy Contributions (Expressed in eV) per PEG Dimer Molecule Binding the TiO_2 (101) Anatase Surface in $D_{010\text{-}cis}$, $D_{101\text{-}f}$, or $D_{br\text{-}AD}$ Configurations, In Low Coverage and Full Coverage Regimes, As Described in Figure 5

	Low Coverage		
	ΔE_{ads}^{mol}	ΔE_{bind}	ΔE_{def}
$D_{010\text{-}cis}$	−1.88	−2.70	0.73
$D_{br\text{-}AD}$	−1.82	−2.00	0.18
$D_{101\text{-}f}$	−0.99	−1.24	0.25
	Full Coverage		
	ΔE_{ads}^{mol}	$\frac{\Delta E_{bind}}{n_{mol}}$	$\frac{\Delta E_{def}}{n_{mol}}$	$\frac{\Delta E_{inter}}{n_{mol}}$
$D_{010\text{-}cis}$	−1.68	−2.26	0.69	−0.11
$D_{br\text{-}AD}$	−1.48	−1.58	0.16	−0.06
$D_{101\text{-}f}$	−1.14	−0.90	0.28	−0.52

DOI: 10.1021/acs.jpcc.6b09554
J. Phys. Chem. C 2016, 120, 29190−29201

configuration is much larger than the one for $D_{br\text{-}AD}$. This could mean that, from a "kinetic" point of view, the bridging $D_{br\text{-}AD}$ adsorption mode should be preferable with respect to the flat $D_{010\text{-}cis}$ adsorption mode.

For the full coverage regime, the situation is more complex. Beyond the energetic contributions already discussed above, there is an additional energy stabilization that the PEG dimer molecules gain from the fact that they are very close one to the other, which is due to the long-range dispersion interactions. We defined this contribution to the total adsorption energy as the intermolecular energy (ΔE_{inter}):

$$\Delta E_{ads}^{mol} = \frac{\Delta E_{bind} + \Delta E_{def} + \Delta E_{inter}}{n_{mol}} \quad (7)$$

The full coverage regime is described in the lower panel of Figure 5 and data are reported in the bottom part of Table 5. We note that, even though the adsorption energy per molecule is still higher for $D_{010\text{-}cis}$ and $D_{br\text{-}AD}$ than for $D_{101\text{-}f}$, the difference is extremely reduced and the energy per adsorption site is higher for the latter (see the last column of the molecular cases in Table 4). With respect to the low coverage regime, the ΔE_{ads}^{mol} for the $D_{010\text{-}cis}$ and $D_{br\text{-}AD}$ is reduced, while for $D_{101\text{-}f}$ it is increased as a consequence of the particularly high intermolecular interaction (ΔE_{inter}) between the adsorbing PEG dimer molecules. This extra energy promotes the standing adsorption for coverage densities beyond a certain threshold.

3.3.2. Dispersion Corrections Evaluation. In this section, we present a more detailed analysis of the dispersion forces contribution to the adsorption energy. This is obtained by calculating the total energies of the optimized structures without the inclusion of the Grimme-D2 van der Waals corrections. The new energies are computed with single-point PBE SCF calculations and reported in Table 2 or 4, depending on the coverage regime considered. The aim of this study is to demonstrate the strict requirement of the semiempirical correction to achieve a better description of the several intra- and intermolecular weak interactions present in the systems under investigation.

We wish to underline that the description of dispersion forces is very delicate, and the method we use here (Grimme-D2) may slightly overestimate the energy associated with dispersion interactions.

For this analysis, both the low and full PEG coverage densities are considered, as in the previous section 3.3.1. The adsorption energies are found to be highly reduced when van der Waals corrections are not included, indicating that a large portion of the interactions (i) between the PEG dimer molecules, (ii) within the PEG dimer molecules themselves, and (iii) between the PEG dimer molecules and the surface come from weak long-range dispersion forces.

At low coverage, when only one molecule is present on the surface, for both $D_{010\text{-}cis}$ or $D_{br\text{-}AD}$ configurations a remarkable reduction of the total adsorption energy value (ΔE_{ads}) is observed, with respect to the case where dispersion corrections are considered (from −1.88 to −0.94 eV and from −1.82 to −1.16 eV, respectively; see Table 2, parenthetical values). This is mainly because, when laying on the surface, the PEG dimer molecule laterally interacts with the surface Ti and O atoms. In the standing $D_{101\text{-}f}$ case, the observed reduction for ΔE_{ads} is lower (from −0.99 to −0.64 eV) because the interaction between the molecule and the surface is smaller if compared to the $D_{010\text{-}cis}$ and $D_{br\text{-}AD}$ cases.

At full coverage, the energy discrepancies are even larger (see Table 4, parenthetical values). For the $D_{010\text{-}cis}$ or $D_{br\text{-}AD}$ configurations, the reduction of adsorption energies (ΔE_{ads}) is from −3.36 to −1.37 eV and from −4.45 to −1.44 eV, respectively. However, the most substantial underestimation is reported for the full coverage standing $D_{101\text{-}f}$ case, where the energy reduction is of ∼72% (from −6.85 to −1.93 eV). In this case, each Ti_{5c} adsorption site hosts a PEG dimer molecule; therefore, the chains are very close one to one another, and thus, many lateral weak interactions are established.

It is noteworthy that, at low coverage density, although the adsorption energies are underestimated, the differences among the adsorption modes are in the correct order. On the contrary, at full coverage density, the obtained noncorrected adsorption energies provide a wrong picture: the three adsorption modes are characterized by similar adsorption energy values, whereas when dispersion forces are taken into account, the standing $D_{101\text{-}f}$ case is largely the most favorable. From this analysis, it is clear that neglecting the dispersion corrections leads not only to a wrong largely underestimated evaluation of the adsorption energy but, in the full coverage regime, also to a qualitatively wrong characterization of the binding mode.

3.4. Comparison between PEG vs Water Adsorption. The adsorption of water on the TiO_2 (101) anatase surface has been widely studied in many theoretical works during the past decade.[18,23−25] In this section, we calculate the adsorption energy of a 1/4 and 1 monolayer (ML) of water on the anatase (101) TiO_2 surface (coverage $\theta = 0.25$ and $\theta = 1.0$), both in the molecular and dissociated configurations (see Figure 6S). Since each water molecule occupies a Ti_{5c} site (thus $\Delta E_{ads}^{mol} = \Delta E_{ads}^{site}$), one molecule represents the 1/4 of a monolayer, with a coverage of 25% and four molecules represent one monolayer, with a coverage of 100%. Furthermore, we compare results obtained for water adsorption, both with and without the inclusion of dispersion corrections, with those obtained for the PEG dimer molecule. This provides a first assessment on the thermodynamic competition for adsorption between the polymer and water, the most common solvent in the human body. The PEG competition for adsorption on the TiO_2 surface with water molecules is a key aspect since in most of the real situations the medium is aqueous.

We first compare the results for water adsorption from the present study with those reported in previous theoretical works (using standard PBE or hybrid PBE0 functionals)[21,42,43] and with data on water adsorption energy from temperature-programmed desorption (TPD) experiments[44] (see Table 6). If dispersion corrections are considered, the adsorption energy results to be slightly overestimated, especially in the case of dissociated water. This comes from the fact that the H-bond between the dissociated H atoms of the water molecule, bonded to the surface O_{2c} atoms, and the OH groups, bonded to the Ti_{5c} sites, is increased by an extra stabilization due to the inclusion of weak interactions.

We first consider the case of an infinite PEG chain, laying on the surface, as described in section 3.1. We notice that the chain folding (as in PEG_{br} in Figure 1c) increases the intramolecular weak interactions and at the same time allows for fitting of the Ti_{5c} pattern of the TiO_2 (101). Only in such conditions, the adsorption energy per site ($\Delta E_{ads}^{site} = -0.98$ eV) is higher than that of water molecules ($\Delta E_{ads}^{mol} = \Delta E_{ads}^{site} = -0.91$ and −0.86 eV at low and full coverage, respectively) and, thus, PEG may bind to the surface; otherwise, (see PEG_{010} and $PEG_{br\text{-}phys}$ in Figure

DOI: 10.1021/acs.jpcc.6b09554
J. Phys. Chem. C 2016, 120, 29190−29201

Table 6. Adsorption Energy (Expressed in eV) per Water Molecule[a]

	Θ	no. of H_2O per cell	% of occ Ti_{5c} sites	ΔE_{ads}^{mol}, H_2O	ΔE_{ads}^{mol}, OH,H
PBE-D2[b]	0.25	1	25	−0.91	−0.53
	1	4	100	−0.86	−0.66
PBE[b]	0.25	1	25	−0.67	−0.29
	1	4	100	−0.62	−0.43
PBE[42]	1	1	25	−0.74	−0.23
	0.25	4	100	−0.72	−0.44
PBE[21]	0.25	1	25	−0.71	−0.38
PBE0[43]	1	4	100	−0.62	
Exp.[44]	1	4	100	−0.50/−0.70	

[a]We considered both molecular H_2O and dissociated OH, H adsorption, at two different coverage densities: a complete monolayer of water, four water molecules on top of four Ti_{5c} sites per supercell (θ = 1) or 1/4 of a monolayer of water, one water molecule on top of one Ti_{5c} site, out of four, per supercell (θ = 0.25). Representations of the optimized structures are reported in Figure 6S. [b]This work.

1a,b) water may cause the polymer desorption, having a larger affinity for the Ti undercoordinated atoms.

Next, we consider the case of the PEG dimer molecules, as described in section 3.2. We recall that at low coverage regime, the most stable configurations are $D_{010\text{-}cis}$ and $D_{br\text{-}AD}$ (the latter, especially, when completely dissociated) and that the bridging $D_{br\text{-}AD}$ could be preferable with respect to $D_{010\text{-}cis}$, because of a lower deformation energy needed to achieve the adsorption configuration (see the discussion in section 3.3.1 and Table 5, upper part). Even if the adsorption energy per molecule (ΔE_{ads}^{mol}) is higher with respect to that for water ($\Delta E_{ads}^{mol} = \Delta E_{ads}^{site}$ = −0.91 eV), for both $D_{010\text{-}cis}$ (−1.88 eV) and $D_{br\text{-}AD}$ (−1.82 eV) the energy per site (ΔE_{ads}^{site}) is, instead, exactly the same for water and $D_{br\text{-}AD}$ (−0.91 eV) and even lower for $D_{010\text{-}cis}$ (−0.63 eV). This means that a competition between PEG and water may occur at this coverage level. When the grafting density increases, the $D_{101\text{-}f}$ configuration becomes more energetically favorable, with a higher value of ΔE_{ads}^{site} (−1.03 eV at 33%, −1.17 eV at 50%, −1.14 eV at 100%), by about −0.2/−0.3 eV, than that for water ($\Delta E_{ads}^{mol} = \Delta E_{ads}^{site}$ = −0.86 eV at full coverage). Under such conditions and for such configurations of the PEG polymers, water cannot induce the PEG desorption.

Cleary, in a real environment, more complex situations could take place, where, for example, water molecules and coating polymers coexist on the surface, interact one with the other, and compete in the adsorption and desorption processes, in strong dependence with the external parameters (e.g., temperature, pressure, pH). Thus, the exact nature of such competitions should be studied in the solvated state, using molecular dynamics techniques based on first-principles or classical potentials. This, however, is beyond the scopes of the present work and will be the subject of future studies.

Furthermore, even if the defect-free surface considered in this work may represent the largest portion of titania surfaces, realistic systems are always imperfect. Defects like steps and kinks, or undercoordinated atoms (e.g., Ti_{4c} and Ti_{3c} presents in TiO_2 nanoparticles[45]) can be expected to alter the adsorption energy of solvent and coating molecules. Therefore, this work is meant as a preliminary investigation on how TiO_2 surfaces behave once exposed to a complex biological environment.

4. CONCLUSIONS

In biomedical applications, TiO_2 nanoparticles are generally coated with polymers to prevent agglomeration, to improve biocompatibility and to reduce their cytotoxicity. Although the synthesis processes of such composite compounds are well established, there is still a big lack of information on the nature of the interaction between the titania surface and the organic macromolecules. In this work, the adsorption of polyethylene glycol (PEG) on the TiO_2 (101) anatase surface was modeled by means of dispersion-corrected density functional theory (DFT-D2) calculations. The two extreme limits of an infinite PEG polymer $[-(OCH_2CH_2)_n]$, on one side, and of a short PEG dimer molecule $[H(OCH_2CH_2)_2OH]$, on the other, were analyzed. Many different molecular configurations and modes of adsorption were compared at increasing surface coverage densities.

An ideally infinite but rippled PEG chain is found to more effectively interact with the surface because, contrary to a stretched PEG chain, it may maximize both the interaction with the surface Ti_{5c} sites and the intramolecular dispersion forces, without paying any cost for distortion.

Short PEG dimer molecules, at both low and medium coverage, prefer to lay on the surface, whereas at full coverage, the adsorption is maximized if the PEG molecules bind perpendicularly to the surface and interact with each other through lateral dispersions, following a mushroom to brush transition, analogous to what experimentally observed for gold surfaces in ref 37, for bioorganic polymeric NPs in ref 46, in general for both organic and inorganic NPs in ref 30, and calculated with a coarse-grained model for hydrophobic surfaces in ref 47. OH dissociated PEG forms are commonly less favored than molecular ones, except when the PEG dimer molecule anchors the surface by binding two Ti_{5c} sites in different rows, thus bridging over an O_{2c}. In this special configuration, an additional strong H-bond is established, providing an extraordinary stabilization for the dissociated forms which become, at low coverage, the most stable among all those considered in this work.

Through the decomposition of the PEG dimer molecule adsorption energy on the TiO_2 surface, it was possible to determine the physical or chemical origin of each contribution. In particular, we determined the cost to deform the molecule from its gas-phase configuration to that adapted for adsorption, the binding energy of the deformed species to the surface, the intramolecular and intermolecular interaction energies. This analysis clearly highlights the fundamental role played by the dispersion forces. Non-dispersion-corrected methods lead not only to a largely underestimated evaluation of the adsorption energies but at full coverage also to a qualitatively wrong characterization of the binding or adsorption mode.

Finally, we considered the adsorption of competing water molecules at different coverage densities. This allows assessing on the stability of PEG in aqueous media. We found out that, at low and medium coverage, PEG and water molecules compete almost on equal, whereas, at full coverage, PEG binds more strongly than water that, therefore, cannot cause its desorption. Further work will be performed in the future in order to accurately model the more complex real environment of PEG coated TiO_2 nanoparticles by considering the effect of temperature, pressure and pH.

DOI: 10.1021/acs.jpcc.6b09554
J. Phys. Chem. C 2016, 120, 29190−29201

■ ASSOCIATED CONTENT

Supporting Information

The Supporting Information is available free of charge on the ACS Publications website at DOI: 10.1021/acs.jpcc.6b09554.

Adsorption energies and optimized structures of molecular and dissociated dimer molecule configurations in the low coverage regime; optimized structures of molecular and dissociated dimer molecule configurations in the medium coverage regime and in the full coverage regime; optimized structures of molecular and dissociated water at $\theta = 0.25$ and $\theta = 1$ (PDF)

■ AUTHOR INFORMATION

Corresponding Authors

*E-mail: daniele.selli@unimib.it. Tel: +390264485235. Fax: +390264485400.

*E-mail: cristiana.divalentin@mater.unimib.it. Tel: +390264485235. Fax: +390264485400.

Notes

The authors declare no competing financial interest.

■ ACKNOWLEDGMENTS

We are grateful to Lara Ferrighi and Gianluca Fazio for many useful discussions and to Lorenzo Ferraro for his technical help. The project has received funding from the European Research Council (ERC) under the European Union's HORIZON2020 research and innovation programme (ERC Grant Agreement No [647020]). TU Dresden-ZIH is acknowledged for CPU time.

■ REFERENCES

(1) Diebold, U. The Surface Science of Titanium Dioxide. *Surf. Sci. Rep.* **2003**, *48*, 53−229.

(2) Buso, D.; Post, M.; Cantalini, D.; Mulvaney, P.; Martucci, A. Gold Nanoparticle-Doped TiO_2 Semiconductor Thin Films: Gas-Sensing Propertie. *Adv. Funct. Mater.* **2008**, *18*, 3843−3849.

(3) Fujishima, A.; Honda, K. Electrochemical Photolysis of Water at a Semiconductor Electrode. *Nature* **1972**, *238*, 37−38.

(4) Shen, G. X.; Du, R. G.; Chen, Y. C.; Lin, C. J.; Scantlebury, D. Study on Hydrophobic Nano-Titanium Dioxide Coatings for Improvement in Corrosion Resistance of Type 316L Stainless Steel. *Corrosion* **2005**, *61*, 943−950.

(5) Bannat, I.; Wessels, K.; Oekermann, T.; Rathousky, J.; Bahnemann, D.; Wark, M. Improving the Photocatalytic Performance of Mesoporous Titania Films by Modification with Gold Nanostructures. *Chem. Mater.* **2009**, *21*, 1645−1653.

(6) Grätzel, M. Photoelectrochemical Cells. *Nature* **2001**, *414*, 338−344.

(7) Zakeeruddin, S. M.; Nazeeruddin, M. K.; Pèchy, P.; Rotzinger, F. P.; Humphry-Baker, R.; Grätzel, M.; Shklover, V.; Haibach, T. Molecular Engineering of Photosensitizers for Nanocrystalline Solar Cells: Synthesis and Characterization of Ru Dyes Based on Phosphonated Terpyridines. *Inorg. Chem.* **1997**, *36*, 5937−5946.

(8) Fujishima, A.; Zhang, X.; Tryk, D. A. TiO_2 Photocatalysis and Related Surface Phenomena. *Surf. Sci. Rep.* **2008**, *63*, 515−582.

(9) Rajh, T.; Dimitrijevic, N. M.; Bissonnette, M.; Koritarov, T.; Konda, V. Titanium Dioxide in the Service of the Biomedical Revolution. *Chem. Rev.* **2014**, *114*, 10177−10216.

(10) Gribb, A. A.; Banfield, J. F. Particle Size Effects on Transformation Kinetics and Phase Stability in Nanocrystalline TiO_2. *Am. Mineral.* **1997**, *82*, 717−728.

(11) Rajh, T.; Dimitrijevic, N. M.; Rozhkova, E. A. Titanium Dioxide Nanoparticles in Advanced Imaging and Nanotherapeutics. *Methods Mol. Biol.* **2011**, *726*, 63−75.

(12) Yamaguchi, S.; Kobayashi, H.; Narita, T.; Kanehira, K.; Sonezaki, S.; Kudo, N.; Kubota, Y.; Terasaka, S. Sonodynamic Therapy Using Water-Dispersed TiO_2-Polyethylene Glycol Compound on Glioma Cells: Comparison of Cytotoxic Mechanism with Photodynamic Therapy. *Ultrason. Sonochem.* **2011**, *18*, 1197−1204.

(13) Yamaguchi, S.; Kobayashi, H.; Narita, T.; Kanehira, K.; Sonezaki, S.; Kubota, Y.; Terasaka, S.; Iwasaki, Y. Novel Photodynamic Therapy Using Water-Dispersed TiO_2-Polyethylene Glycol Compound: Evaluation of Antitumor Effect on Glioma Cells and Spheroids in Vitro. *Photochem. Photobiol.* **2010**, *86*, 964−971.

(14) Oberdorster, G.; Ferin, J.; Gelein, R.; Soderholm, S. C.; Finkelstein, J. Role of the Alveolar Macrophage in Lung Injury: Studies with Ultrafine Particles. *Environ. Health Perspect.* **1992**, *97*, 193−199.

(15) Hamzeh, M.; Sunahara, G. I. In Vitro Cytotoxicity and Genotoxicity Studies of Titanium Dioxide (TiO_2) Nanoparticles in Chinese Hamster Lung Fibroblast Cells. *Toxicol. In Vitro* **2013**, *27*, 864−873.

(16) Mano, S. S.; Kanehira, K.; Sonezaki, S.; Taniguchi, A. Effect of Polyethylene Glycol Modification of TiO_2 Nanoparticles on Cytotoxicity and Gene Expressions in Human Cell Lines. *Int. J. Mol. Sci.* **2012**, *13*, 3703−3717.

(17) Lazzeri, M.; Vittadini, A.; Selloni, A. Structure and Energetics of Stoichiometric TiO_2 Anatase Surfaces. *Phys. Rev. B: Condens. Matter Mater. Phys.* **2001**, *63*, 155409.

(18) Selloni, A.; Vittadini, A.; Grätzel, M. The Adsorption of Small Molecules on the TiO_2 Anatase (101) Surface by First-Principles Molecular Dynamics. *Surf. Sci.* **1998**, *402*−*404*, 219−222.

(19) Di Valentin, C.; Costa, D. Anatase TiO_2 Surface Functionalization by Alkylphosphonic Acid: A DFT+D Study. *J. Phys. Chem. C* **2012**, *116*, 2819.

(20) Tilocca, A.; Selloni, A. Methanol Adsorption and Reactivity on Clean and Hydroxylated Anatase (101) Surfaces. *J. Phys. Chem. B* **2004**, *108*, 19314−19319.

(21) Li, W.-K.; Gong, X.-Q.; Lu, G.; Selloni, A. Different Reactivities of TiO_2 Polymorphs: Comparative DFT Calculations of Water and Formic Acid Adsorption at Anatase and Brookite TiO_2 Surfaces. *J. Phys. Chem. C* **2008**, *112*, 6594−6596.

(22) Di Valentin, C.; Fittipaldi, D. Hole Scavenging by Organic Adsorbates on the TiO_2 Surface: A DFT Model Study *J. Phys. J. Phys. Chem. Lett.* **2013**, *4*, 1901−1906.

(23) Tilocca, A.; Selloni, A. Vertical and Lateral Order in Adsorbed Water Layers on Anatase TiO_2(101). *Langmuir* **2004**, *20*, 8379−8384.

(24) Sumita, M.; Hu, C.; Tateyama, Y. Interface Water on TiO_2 Anatase (101) and (001) Surfaces: First-Principles Study with TiO_2 Slabs Dipped in Bulk Water. *J. Phys. Chem. C* **2010**, *114*, 18529−18537.

(25) Vittadini, A.; Selloni, A.; Rotzinger, F. P.; Grätzel, M. Formic Acid Adsorption on Dry and Hydrated TiO_2 Anatase (101) Surfaces by DFT Calculations. *J. Phys. Chem. B* **2000**, *104*, 1300−1306.

(26) Monti, S.; van Duin, A. C. T.; Kim, S. Y.; Barone, V. Exploration of the Conformational and Reactive Dynamics of Glycine and Diglycine on TiO_2: Computational Investigations in the Gas Phase and in Solution. *J. Phys. Chem. C* **2012**, *116*, 5141−5150.

(27) Szieberth, D.; Ferrari, A. M.; Dong, X. Adsorption of Glycine on the Anatase (101) Surface: an *Ab Initio* Study. *Phys. Chem. Chem. Phys.* **2010**, *12*, 11033−11040.

(28) Agosta, L.; Zollo, G.; Arcangeli, C.; Buonocore, F.; Gala, F.; Celino, M. Water Driven Adsorption of Amino Acids on the (101) Anatase TiO_2 Surface: an Ab Initio Study. *Phys. Chem. Chem. Phys.* **2015**, *17*, 1556−1561.

(29) Carravetta, V.; Monti, S. Peptide-TiO_2 Surface Interaction in Solution by Ab Initio and Molecular Dynamics Simulations. *J. Phys. Chem. B* **2006**, *110*, 6160−6169.

(30) Jokerst, J. V.; Lobovkina, T.; Zare, R. N.; Gambhir, S. S. Nanoparticle PEGylation for Imaging and Therapy. *Nanomedicine* **2011**, *6*, 715−728.

(31) Matsumura, S.; Sato, S.; Yudasaka, M.; Tomida, A.; Tsuruo, T.; Iijima, S.; Shiba, K. Prevention of Carbon Nanohorn Agglomeration

DOI: 10.1021/acs.jpcc.6b09554
J. Phys. Chem. C 2016, 120, 29190−29201

Using a Conjugate Composed of Comb-Shaped Polyethylene Glycol and a Peptide Aptamer. *Mol. Pharmaceutics* **2009**, *6*, 441−447.
(32) Salmaso, S.; Caliceti, P. Stealth Properties to Improve Therapeutic Efficacy of Drug Nanocarriers *J. J. Drug Delivery* **2013**, *2013*, 1−19.
(33) Schöttler, S.; Becker, G.; Winzen, S.; Steinbach, T.; Mohr, K.; Landfester, K.; Mailänder, V.; Wurm, F. R. Protein Adsorption is Required for Stealth Effect of Poly(Ethylene Glycol)- and Poly-(Phosphoester)-Coated Nanocarriers. *Nat. Nanotechnol.* **2016**, *11*, 372−377.
(34) Wang, W.; Xiong, W.; Wan, J.; Sun, X.; Xu, H.; Yang, X. The Decrease of PAMAM Dendrimer-Induced Cytotoxicity by PEGylation via Attenuation Ofoxidative Stress. *Nanotechnology* **2009**, *20*, 105103−105109.
(35) Prencipe, G.; Tabakman, S. M.; Welsher, K.; Liu, Z.; Goodwin, A. P.; Zhang, L.; Henry, J.; Dai, H. PEG Branched Polymer for Functionalization of Nanomaterials with Ultralong Blood Circulation. *J. Am. Chem. Soc.* **2009**, *131*, 4783−4787.
(36) Grimme, S. Semiempirical GGA-type Density Functional Constructed with a Long-Range Dispersion Correction. *J. Comput. Chem.* **2006**, *27*, 1787−1799.
(37) Backmann, N.; Kappeler, N.; Braun, T.; Huber, F.; Lang, H.-P.; Gerber, C.; Lim, R. Y. H. Sensing Surface PEGylation with Microcantilevers. *Beilstein J. Nanotechnol.* **2010**, *1*, 3−13.
(38) Perdew, J. P.; Burke, K.; Ernzerhof, M. Generalized Gradient Approximation Made Simple. *Phys. Rev. Lett.* **1996**, *77*, 3865−3868.
(39) Vanderbilt, D. Soft Self-Consistent Pseudopotentials in a Generalized Eigenvalue Formalism. *Phys. Rev. B: Condens. Matter Mater. Phys.* **1990**, *41*, 7892−7895.
(40) Giannozzi, P.; Baroni, S.; Bonini, N.; Calandra, M.; Car, R.; Cavazzoni, C.; Ceresoli, D.; Chiarotti, G. L.; Cococcioni, M.; Dabo, I.; et al. QUANTUM ESPRESSO: a Modular and Open-Source Software Project for Quantumsimulations of Materials. *J. Phys.: Condens. Matter* **2009**, *21*, 395502−395521.
(41) Dumont, E. L. P.; Belmas, H.; Hess, H. Observing the Mushroom-to-Brush Transition for Kinesin Proteins. *Langmuir* **2013**, *29*, 15142−15145.
(42) Vittadini, A.; Selloni, A.; Rotzinger, F. P.; Grätzel, M. Structure and Energetics of Water Adsorbed at TiO_2 Anatase (101) and (001) Surfaces. *Phys. Rev. Lett.* **1998**, *81*, 2954−2957.
(43) Chang, J.-G.; Wang, J.; Lin, M. C. Adsorption Configurations and Energetics of BCl_x (x = 0−3) on TiO_2 Anatase (101) and Rutile (110) Surfaces. *J. Phys. Chem. A* **2007**, *111*, 6746−6754.
(44) Egashira, M.; Kawasumi, S.; Kagawa, S.; Seiyama, T. Temperature Programmed Desorption Study of Water Adsorbed on Metal Oxides. *Bull. Chem. Soc. Jpn.* **1978**, *51*, 3144−3149.
(45) Fazio, G.; Ferrighi, L.; Di Valentin, C. Spherical versus Faceted Anatase TiO_2 Nanoparticles: A Model Study of Structural and Electronic Properties. *J. Phys. Chem. C* **2015**, *119*, 20735−20746.
(46) Xu, Q.; Ensign, L. M.; Boylan, N. J.; Schön, A.; Gong, X.; Yang, J. C.; Lamb, N. W.; Cai, S.; Yu, T.; Freire, E.; et al. Impact of Surface Polyethylene Glycol (PEG) Density on Biodegradable Nanoparticle Transport in Mucus Ex Vivo and Distribution in Vivo. *ACS Nano* **2015**, *9*, 9217−27.
(47) Lee, H.; de Vries, A. H.; Marrink, S. T.; Pastor, R. W. A Coarse-Grained Model for Polyethylene Oxide and Polyethylene Glycol: Conformation and Hydrodynamics. *J. Phys. Chem. B* **2009**, *113*, 13186−13194.

DOI: 10.1021/acs.jpcc.6b09554
J. Phys. Chem. C 2016, 120, 29190−29201